*Short communication*

# Novel $Fe_{70}Zr_{10}Ni_6Al_4Si_6B_4$ thick metallic glass coating produced by laser cladding

X. L. Wu and Y. S. Hong

**A novel multicomponent thick metallic glass coating has been synthesised by laser cladding. The maximum coating thickness was 1 mm. The clad cooling rate restrained the epitaxial growth of dendrites in the metallic glass coating. The metallic glass had high glass forming ability with a wide supercooled liquid region ranging from 59 to 70 K. The metallic glass coating also revealed high hardness and good corrosion resistance. MST/4765**

*At the time the work was carried out the authors were in the State Key Laboratory of Nonlinear Mechanics, Institute of Mechanics, Chinese Academy of Sciences, Beijing 100080, China. Dr Wu is now in the Chemical Engineering Department, Cleveland State University, 1960 E24th St, SH455, Cleveland, OH44115–2425, USA (wuxl_cas@hotmail.com).* *Manuscript received 17 July 2000; accepted 17 January 2001.*


## Introduction

Laser processing of metallic glass layers has been of long standing interest. However, laser application of most metallic glass layers has required high cooling rates above $10^5$ K $s^{-1}$ and the resulting layer thickness has been limited to less than 50 μm. In the mid 1990s, novel bulk metallic glasses were produced.[1,2] Distinct from conventional metallic glass, the novel bulk materials were of multicomponent chemistry and had high stability with respect to crystallisation in the supercooled liquid region and highly dense, randomly packed structures that led to excellent glass forming ability.[1–8] A series of Zr, Mg, La, Pd, Ti, and Fe based bulk metallic glasses having excellent mechanical and physical properties were fabricated.

With the aim of eliminating the limitation of critical layer thickness, and of obtaining the required novel structure and high glass forming ability, the production of a multicomponent Fe based metallic glass coating by laser cladding is discussed.

## Experimental

An AISI 1045 steel plate, 40 mm in length, 30 mm in width, and of 20 mm thickness was used as the substrate. The composition of the steel was Fe–0·43C–0·21Si–0·35Mn–$\leqslant$0·02P–$\leqslant$0·04S (all wt-%). The clad alloy was a multicomponent $Fe_{70}Zr_{10}Ni_6Al_4Si_6B_4$ (at.-%) powder mixture. The powder particles were from 6 to 44 μm in size and powder purity ranged from 99·95 to 99·99 wt-%. The powders were mixed evenly in an argon gas atmosphere and then pasted on the substrate surface to a thickness of $\sim$1 mm.

A 10 kW CW $CO_2$ laser was used to produce the coating. The technique of laser cladding was adopted because this process has only a small volumetric dilution ratio and hence the alloy elements of the substrate have little influence upon the composition of the coating. The laser was operated at power of 7·5 kW, beam diameter of 4·5 mm, and process speed of 40 mm $s^{-1}$. After allowing argon gas to flow through the shielding box for 10 min, laser cladding was carried out under continuous high purity argon gas shielding, a beam of argon gas being allowed to flow over the processing region.

The coating was characterised using energy dispersive X-ray spectrometry (Link AN1000 EDS with a detecting error of less than 0·5%), X-ray diffractometry (Rigaku XRD, *D*/max-RB, 12 kW, Co $K_\alpha$ radiation), optical microscopy (Neuphot-21), and transmission electron microscopy (Philips EM420 TEM). The thermal stability associated with the glass transition, supercooled liquid, and crystallisation was examined at a heating rate of 0·17 K $s^{-1}$ using differential scanning calorimetry (Perkin-Elmer DSC with an energy sensitivity of 0·02 mJ $s^{-1}$). The melting temperature $T_m$ was ascertained by differential thermal analysis. Thin slices taken parallel to the top surface of the substrate were obtained for XRD, DSC, and TEM analysis using a slow speed cut-off saw set to a thickness of 100 μm. Successive cuts assured inspection of the entire coating at specific depths. The dimensions of the final DSC sample were 10 mm × 5 mm × 50 μm. Film samples for TEM were prepared by mechanical thinning to 50 μm, followed by chemical polishing in a solution of 35 vol.-% nitric acid and 65 vol.-% methanol at 25 K below zero. Microhardness was measured using a Vickers hardness tester under a 200 g load. Corrosion resistance was analysed by measuring the weight loss after immersion in aqua regia for 1·8 ks at 297 K.

## Results

The distribution of clad elements close to the coating/substrate bond region is shown in Fig. 1. A uniform distribution of elements can be seen in the coating. There is also some degree of dilution of alloy elements at the coating/substrate interface.

The morphology of the cross-section of the coating, heat affected zone, and substrate, as observed by low magnification optical microscopy, is shown in Fig. 2*a*. The coating has a maximum thickness of about 1 mm. High magnification (Fig. 2*b*) of the coating/HAZ bond region reveals that initially there is some epitaxial growth of dendrites at the coating/substrate interface which is subsequently completely suppressed in the coating. The coating revealed featureless contrast on etching with hydrofluoric acid or aqua regia. No contrast indicates a crystalline phase.

The XRD pattern 0·3 mm from the top surface of the coating is shown in Fig. 3. Only a broad halo peak can be seen: no diffraction peak corresponding to a crystalline phase can be observed. The bright field TEM image of the microstructure 0·3 mm from the top surface of the coating, shown in Fig. 4, confirms the absence of any crystalline phase: the inset selected area diffraction pattern consists of halo rings typical of a metallic glass. A number of XRD and TEM observations made at various coating depths showed

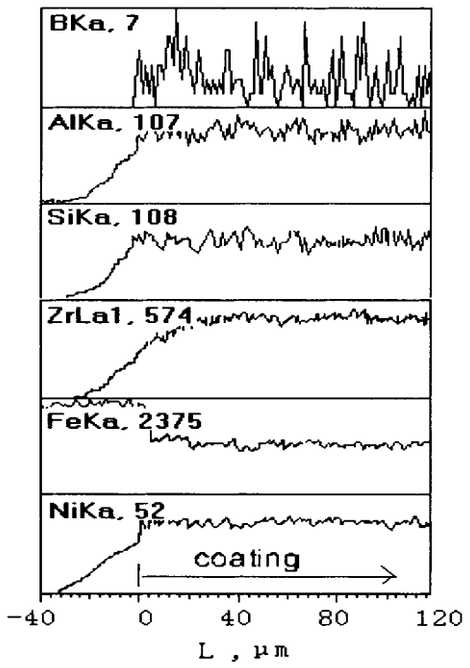


**1 Distribution of alloy elements of clad coating obtained by EDS: numbers represent relative concentrations**

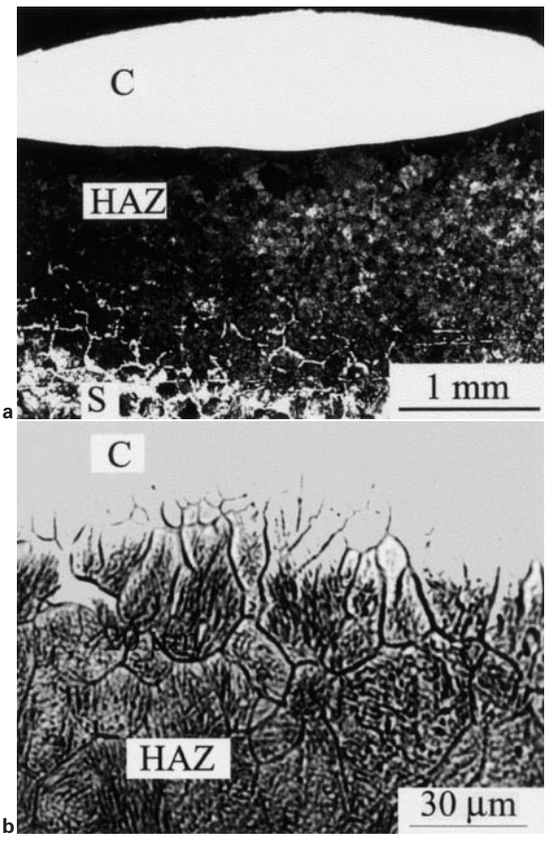


*a* low magnification; *b* high magnification of coating/substrate bond region

**2 Optical micrographs of cross-section of coating (C coating, HAZ heat affected zone, S substrate)**

the same results. Therefore, the clad cooling rate is high enough to suppress precipitation of the crystalline phase and to produce metallic glass.

The DSC curve of the metallic glass, 0·2 mm from the top surface of the coating, is shown in Fig. 5. The glass transition temperature $T_g$ and the temperature at which crystallisation starts $T_x$ are marked on the figure. The temperature interval $\Delta T_x = T_g - T_x$ is the supercooled liquid region. The variations of $T_g$, $T_x$, melting temperature $T_m$, $\Delta T_x$, and reduced temperature $T_g/T_m$ with coating depth are given in Table 1. It can be seen that both $T_g$ and $T_x$ increase monotonically when approaching the top surface of the coating. However, the incremental increase is greater for $T_x$ than for $T_g$: therefore, $\Delta T_x$ increases. At each depth, there is a wide supercooled liquid region $\Delta T_x$ which ranges from 59 to 70 K. In addition, $T_g/T_m$ values are between 0·6 and 0·68. The present values of both $\Delta T_x$ and $T_g/T_m$ are very similar to those of other Fe based bulk metallic glasses.[3–6] Wide supercooled liquid region implies high thermal stability of the supercooled liquid with respect to crystallisation. Furthermore, the larger the $T_g/T_m$ ratio, the greater the glass forming ability. There is a clear tendency for glass forming ability to increase with increasing $\Delta T_x$ and $T_g/T_m$.[1,5,6] High glass forming ability allows the fabrication of a thick metallic glass coating.

The hardness of the coating was as high as 1020 HV0·2 and no weight loss was detected after immersion in aqua regia for 1·8 ks at 297 K. Therefore, the thick metallic glass coating possesses simultaneously high glass forming ability, high hardness, and high corrosion resistance.

## Discussion

The base composition of the present thick metallic glass coating lies in the Fe–Zr–B system; it satisfies the following three empirical rules:[1] (i) a multicomponent system consisting of more than three constituent elements, (ii) significantly different atomic size ratios above about 13% among the three main constituent elements, and (iii) large negative heats of mixing of the main constituent elements. The addition of Al, Si, and Ni increases the degree of agreement with these empirical rules.[1,5] That is, the addition of these elements causes a sequential change in the atomic size in the order $Zr \gg Al > Si > Fe > Ni \gg B$, as well as the generation of new atomic pairs with various negative heats of mixing. The high glass forming ability of the novel thick metallic glass can be discussed in terms of structural, thermodynamic, and kinetic factors.

From the structural point of view, the novel metallic glass has two features that are distinct from conventional metallic

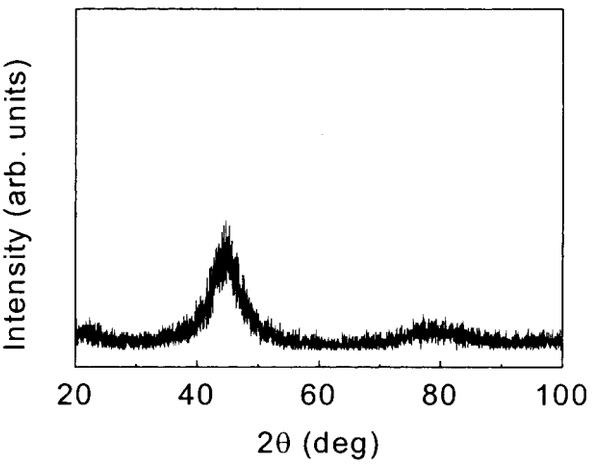


**3 X-ray diffraction pattern 0·3 mm from coating surface**

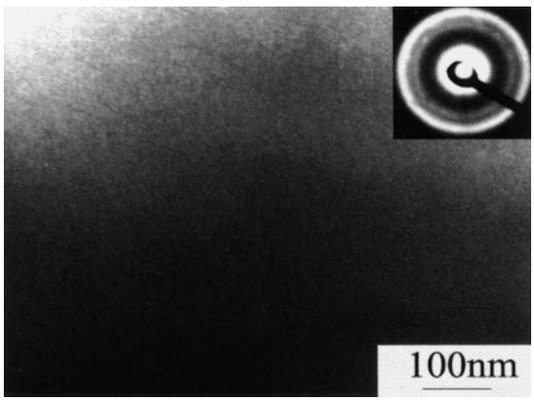


**4 Bright field transmission electron micrograph of morphology of metallic glass 0·3 mm from coating surface: inset shows halo ring diffraction pattern**

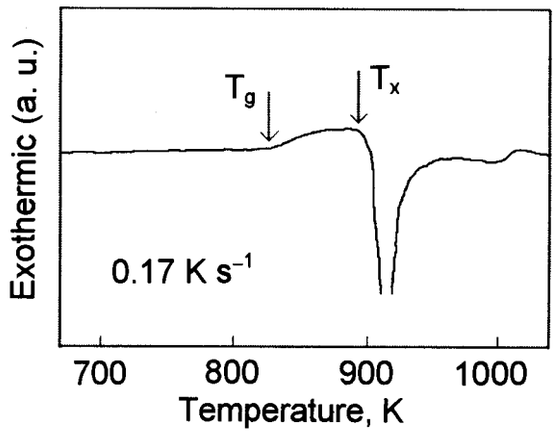


**5 DSC curve of metallic glass 0·2 mm from coating surface: $T_g$ is glass transition temperature and $T_x$ is temperature at which crystallisation starts**

glass:[1,2,7,8] a highly dense, randomly packed structure and significant differences in structure and composition compared to the corresponding crystalline compounds. These two features result from the high order multicomponent alloy system with very different atomic sizes among the constituent elements.

The novel metallic glass consists of elements with significantly different atomic sizes: the atomic size ratios among the three main constituent elements exceeds 13%. The atomic sizes of the constituent elements can be classified into three groups: large, intermediate, and small. Such significant differences in atomic size are expected to cause an increase in the packing density of the supercooled liquid resulting in high liquid/solid interfacial energy.[1,8] The formation of such highly dense randomly packed structures has been widely confirmed.[1,8,9] For conventional metallic glass, there is a difference of local structure between the metallic glass and its liquid state.[10,11] However, using the reduced density function determined by electron diffraction intensity[8] and the X-ray interference function[9] it has been shown that the novel metallic glass is closely analogous to its corresponding liquid phase. The results demonstrate that the novel metallic glass can be regarded as a glass formed continuously from its liquid state at a lower cooling rate: the local structure of the novel metallic glass is more close packed than that of conventional metallic glass.[1,8] In the supercooled liquid region where the three empirical rules are well satisfied, the topological and chemical short range orderings are enhanced, leading to the formation of a highly dense randomly packed structure with low atomic diffusivity. Therefore, it is concluded that the novel metallic glass has a structure similar to its corresponding liquid state. The highly dense, randomly packed structure of the novel metallic glass results from the large atomic size ratios of its multicomponent composition.[1,2]

The local atomic configuration of short range order in conventional metallic glass with poor glass forming ability resembles the corresponding equilibrium compounds with a composition near that of the metallic glass.[11–13] The similarity between the metallic glass and crystalline phase is a fairly general structural feature of early conventional metallic glass.[14] In contrast, the local atomic arrangement in the novel metallic glass is markedly different from that of the corresponding crystalline compounds. A large composition difference exists between the novel metallic glass and the corresponding crystalline compounds.[3–8] Decomposition takes place only in an alloy where its composition is far from the corresponding crystalline compound. Therefore, there are no structural and compositional similarities between the novel metallic glass and its corresponding crystalline compound.

The glass forming ability of metallic glass is closely related to atomic structure. The structural features of the novel bulk metallic glass make the nucleation and growth of crystalline phases from the initially homogeneous supercooled liquid extremely difficult, because of the extremely slow mobility of the constituents in the highly viscous supercooled liquid.[1,2,8] It is very difficult for the six elements in the alloy to satisfy simultaneously the compositional and structural requirements of the crystalline compounds. Therefore, the disordered liquid structure of the melt can be frozen with a low cooling rate, which then leads to high glass forming ability. Also, the highly random close packed structure and high viscosity make the redistribution of atoms on a large range scale extremely difficult.[1,8] The greater the number of components of the alloy, the more difficult it is for all constituents to satisfy simultaneously the local structural and compositional requirements of crystalline phases. This argument is known as 'the confusion principle'.[15]

From the thermodynamic point of view, the lower the free energy $\Delta G = \Delta H_f - T\Delta S_f$ for transformation of liquid to crystalline phase, the larger the glass forming ability.[1,16] Here, $\Delta H_f$ and $\Delta S_f$ are the enthalpy of fusion and entropy of fusion, respectively. Low values of $\Delta G$ are obtained in the case of low $\Delta H_f$ and high $\Delta S_f$. The multicomponent alloy system can increase $\Delta S_f$ because $\Delta S_f$ is proportional to the number of configurations of the system. The free energy at constant temperature also decreases in the case of low chemical potential caused by low enthalpy and high reduced glass transition temperature as well as of high interfacial energy between the liquid and solid phase $\sigma_{sl}$. Based on thermodynamic factors, it is concluded that the multiplicity of alloy components which leads to the increase in $\Delta S_f$ causes the more highly dense random packing which is favourable for the decrease in $\Delta H_f$ and the increase in $\sigma_{sl}$.

From the kinetic point of view, the homogeneous nucleation rate $I$ ($cm^3\ s^{-1}$) and linear growth rate $U$

**Table 1 Thermal stability of metallic glass coating**

| Distance, mm | $T_g$, K | $T_x$, K | $\Delta T_x$, K | $T_m$, K | $T_g/T_m$ |
|---|---|---|---|---|---|
| 0·2 | 822 | 892 | 70 | 1209 | 0·68 |
| 0·4 | 818 | 884 | 66 | 1278 | 0·64 |
| 0·6 | 815 | 874 | 59 | 1358 | 0·6 |

$T_g$ is glass transition temperature, $T_x$ is temperature at which crystallisation starts, $\Delta T_x$ ($=T_g-T_x$) is supercooled liquid region, $T_m$ is melting temperature.

(cm $s^{-1}$) of a crystalline phase having a spherical morphology from supercooled liquid can be expressed as[17]

$$I = k'/\eta \exp\{-b\alpha^3\beta/T_r(1-T_r)^2\} \quad (1)$$

$$U = k''/\eta[1-\exp\{-\beta(1-T_r)/T_r\}] \quad (2)$$

where $k'$ and $k''$ are constants, $T_r = T/T_m$ is the reduced temperature, $b$ is the shape factor, $\eta$ is the viscosity, $f$ is the fraction of nucleation sites at the growth interface, and $\alpha$ and $\beta$ are dimensionless parameters that can be expressed as

$$\alpha = (N_0 V^2)^{1/3}\, \sigma_{sl}/\Delta H_f \quad (3)$$

$$\beta = \Delta S_f/RT_m \quad (4)$$

where $N_0$ is Avogadro's number, $V$ is the atomic volume, and $R$ is the gas constant.

The highly random close packed structure of the novel metallic glass may increase $\eta$ greatly. The significant differences in atomic size among the components of the alloy system result in an increase in both $\alpha$ and $\beta$.[1] Changes in $\eta$, $\alpha$, and $\beta$ cause decreases in $I$ and $U$, leading to an increase in glass forming ability. The increases in $\alpha$ and $\beta$ also imply an increase in $\sigma_{sl}$ and in $\Delta S_f$ and a decrease in $\Delta H_f$, being consistent with the thermodynamic interpretation of the achievement of high glass forming ability.

## Conclusions

1. The novel $Fe_{70}Zr_{10}Ni_6Al_4Si_6B_4$ metallic glass coating can be synthesised by laser surface cladding, to a maximum thickness of 1 mm.

2. The metallic glass possesses a high glass forming ability. The supercooled liquid region $\Delta T_x$ extends from 59 to 70 K and the reduced temperature $T_g/T_m$ ranges from 0·6 to 0·68.

3. The metallic glass coating reveals high hardness and good corrosion resistance.

## Acknowledgements

This research was supported by the National Natural Science Foundation (grant no. 19891180), the National Outstanding Youth Scientific Award of China (grant no.19525205), and The Chinese Academy of Sciences.

## References

1. A. INOUE: *Mater. Trans., JIM*, 1995, **36**, 866.
2. W. L. JOHNSON: *Mater. Sci. Forum*, 1996, **225–227**, 35.
3. A. INOUE and J. S. GOOK: *Mater. Trans., JIM*, 1996, **37**, 32.
4. A. INOUE, Y. SHINOHARA, and J. S. GOOK: *Mater. Trans., JIM*, 1995, **36**, 1427.
5. A. INOUE, T. ZHANG, and A. TAKEUCHI: *Appl. Phys. Lett.*, 1997, **71**, 464.
6. A. INOUE, H. KOSHIBA, T. ZHANG, and A. MAKINO: *J. Appl. Phys.*, 1998, **83**, 1967.
7. W. H. WANG, Q. WEI, S. FRIEDRICH, M. P. MACHT, N. WANDERKA, and H. WOLLENBERGER: *Appl. Phys. Lett.*, 1997, **71**, 1053.
8. W. H. WANG, Z. X. BAO, C. X. LIU, D. Q. ZHAO, and J. ECKERT: *Phys. Rev. B.*, 2000, **61**, 3166.
9. E. MATSUBARA, T. TAMURA, Y. WASEDA, A. INOUE, M. KOHINATA, and T. MASUMOTO: *Mater. Trans., JIM*, 1990, **31**, 228.
10. Y. WASEDA: 'The structure of the non-crystalline materials liquid and amorphous solids', 67; 1980, New York, McGraw-Hill.
11. R. WANG: *Nature*, 1979, **278**, 700.
12. C. N. J. WAGNER: *J. Non-Cryst. Solids*, 1992, **150**, 1.
13. K. SUZUKI: *J. Phys., Condens. Matter*, 1991, **3**, F39.
14. S. SINKLER, C. MICHAELSEN, and R. BORMANN: *Phys. Rev. B*, 1997, **55**, 2874.
15. A. L. GREER: *Nature*, 1993, **366**, 303.
16. H. A. DAVIES: 'Amorphous metallic alloys', (ed. F. E. Luborsky), 14; 1983, London, Butterworths.
17. D. TURNBULL: *Solid State Phys.*, 1956, **3**, 225.